Capacitance transient spectroscopy models of coupled trapping kinetics among multiple defect states: Application to the study of trapping kinetics of defects in heavy-ion-damaged silicon

P. K. Giri*

Materials Science Division, Indira Gandhi Centre for Atomic Research, Kalpakkam 603102, India

Y. N. Mohapatra

Department of Physics, Institute of Technology, Kanpur 208016, India

We have considered five different models of charge transfer among coupled defect states in semiconductors where the free-carrier density is limited by the density of unoccupied trap levels, as in the case of defect-dominated materials. To determine the time dependence of the trap occupancy features, we formulate a set of coupled differential equations that govern charge capture and emission processes for two defect states. A numerical solution assuming model parameters for traps provides features of the trap occupancy as a function of time. A critical comparison is made in occupancy features for different models, primarily categorized as serial (hierarchical) and parallel mechanisms of charge transfer. The model predictions are successfully applied to a study of trapping kinetics of defects observed in heavily damaged n-type silicon. We show that, in addition to the occurrence of charge redistribution among multiple traps, the major trap in the damaged silicon exists in two metastable configurations, perhaps with negative U (Hubbard correlation energy), and the stable configuration refers to a midgap compensating center related to a small cluster of self-interstitials. The applicability of our model simulations can be extended to more complex defect systems using a combination of these simple models.

I. INTRODUCTION

Deep electronic states induced by defects in crystalline semiconductors have been extensively studied through the use of capacitance transient spectroscopic techniques such as deep-level transient spectroscopy (DLTS)[1] and its many variants.[2] More recently, an isothermal spectroscopic technique called time-analyzed transient spectroscopy (TATS)[3] has been demonstrated to be advantageous in comparison to the conventional DLTS technique, especially where the interpretation of the DLTS spectra is questionable due to its inherent limitation of being a temperature scanning technique. Both these techniques are based on variations of the capacitance of a diode as a measure of the number of charges trapped within its space-charge region. These techniques primarily allow a determination of important defect parameters such as defect concentration, energy level, thermal capture cross section, defect profile etc. Moreover, the behavior of the spectral line shape as a function of the filling pulse duration can provide additional information on the defect geometry, the structure of metastable defects,[4,5] coupling among defect states,[6] the distinction between pointlike and extended defects,[7] etc.

Standard DLTS analysis for a pointlike defect assumes that the capacitance transient associated with electron emission obeys an exponential decay law. However, multiply charged defects yield DLTS spectra that are often difficult to interpret. These difficulties arise from the multistep kinetics of carrier capture at these traps and of their nonexponential emissions. The problem becomes even more complicated if one of the defect charge states is metastable or strongly coupled to the lattice. Therefore, large lattice relaxation and thermal barriers for capture have to be taken into account in any satisfactory description of spectra related to these deep-level defects. Many important defects in semiconductors exhibit metastable behavior[8] and a majority of these defects is found to have interstitial character.[9] However, very few such defects have been identified and understood so far in terms of fundamental characteristics and the physical mechanism causing the conversion from a stable to a metastable configuration. Coupling among metastable defects has been invoked in many physical systems to account for the observed occupancy features in studies involving depletion layer spectroscopy. Various cases of charge-state-controlled metastable defects have been reported in the literature,[10–13] and their origin ascribed to various causes such as strong coupling to the lattice, negative U (Hubbard correlation energy), and entropy-driven spontaneous changes in configuration.[11] Multiphonon recombination at defects with large lattice relaxation[14] has been proposed to stimulate metastability in the case of compound semiconductors. From recent studies on the metastability of carbon-related defects and the S-Cu complex in Si, it has been concluded that excitonic Auger capture is an important mechanism for configurational change of metastable defects.[15]

Defects with an unusual dependence of the DLTS line shape on the filling pulse width have been reported in several studies.[12,16] Hummelgen and Schroter observed deformation-induced defects in p-CdTe whose DLTS spectra show a decrease in amplitude with an increasing filling pulse width. A similar behavior was observed in n-type $Hg_yCd_{1-y}Te$ by Barbot *et al.*[13] Their samples, containing dislocation loops

generated by ion implantation, showed two peaks with an unusual dependence between their amplitudes and filling pulse width. Many of the reported results present an incomplete interpretation of the spectra due to a lack of proper models of coupling mechanisms and inherent limitations of the respective techniques used. A general formalism for treating the coupled trapping kinetics among multiple states would enable one to understand and isolate the nature of coupling and possible metastable behavior of defects.

In this paper, we first analyze various models of coupling among defect states and the corresponding charge-transfer mechanisms by solving kinetic equations to obtain the distinguishing features of trap occupancy as a function of time. Significant characteristics so obtained are used for model distinction in real systems. We successfully apply our model to unravel the coupling mechanism among multiple traps observed in ion-damaged silicon. A critical comparison of experimental and theoretical occupancy features suggests the involvement of a defect with two different configurations. It is also emphasized that isothermal spectroscopic method such as TATS should be preferred over the conventional DLTS technique to correctly analyze trap occupancy features.

II. MODELS OF CHARGE TRANSFER AMONG COUPLED DEFECT STATES

In a typical capacitance transient measurement, the traps are filled with charge by collapsing the depletion region during a filling-pulse time (t_f), and emptied during a relaxation time (t_r) what is usually measured is the magnitude of the capacitance transient during trap emptying. In trapping kinetics studies, for a simple point defect, the trap occupancy monotonically increases with increasing filling time (t_f), and finally reaches saturation for longer filling times. In such a case, the change in trap occupancy for different filling times follows a semilogarithmic plot. However, complications arise in the presence of multiple states which may be coupled through different mechanisms. A simple way to classify different coupling mechanisms is by noting whether such charge transfers are serial (hierarchical) or parallel. In the case of a serial coupling, the occupancy of the states proceeds sequentially from one localized state to another. In contrast, for parallel coupling, such transfers are indirect and are mediated by the bands, for example by a recapture of carrier into a slow emitting state after emission from a fast emitting state.[17] In a real system of defects, there can also be many combinations of such serial and parallel processes.

Here we will consider five simple models of coupled kinetics among multiple states for a detailed analysis. In order to make a comparative study of different models, we first formulate their kinetic equations and use numerical simulations to obtain their occupancy features, which is usually obtained from typical variable filling-pulse-width experiments. In the first two models, the charge transfer is serial in nature, while in the latter three it is parallel in nature. For simplicity, we have considered models with only two states. These states are assumed to be of donor type, and free carriers are supplied by the ionization of these states. This latter assumption is important in controlling the carrier dynamics of trapping and detrapping, and for compensated material

this condition is naturally satisfied. The physical characteristics of each of these models are briefly presented below.

A. Internal conversion

Here we consider two states which can have conversion from shallow to deep states. While the shallow state has a small barrier to capture, the deep state has a large barrier and cannot localize an electron directly from the conduction band. Both states, however, emit carriers to the conduction band. A schematic of this model is shown in Fig. 1(A), with levels 1 and 2 showing relevant charge states after capture and emission. The corresponding kinetic equations governing their occupancy can be written as

$$\dot{n}_1 = -e_1 n_1 - e_{12} n_2 + c_1 n (1 - n_1 - n_2), \tag{1}$$

$$\dot{n}_2 = e_{12} n_1 - e_2 n_2, \tag{2}$$

with a crucial constraint on the number of electrons as

$$n = 1 - n_1 - n_2. \tag{3}$$

n_1 and n_2 refer to the concentration of filled levels, n is the free-electron concentration, e_1 and e_2 are their respective emission rates, and e_{12} is the rate of conversion from state 1 to state 2. Note that in the equations above, we have normalized all concentrations by the total trap concentration (N_T), for ease of calculations. The normalizing factor N_T is included in the capture coefficient c_1, and this convention is followed in all subsequent discussion.

The effective emission rate of states 1 and 2 can be given by

$$e_1' = e_1 + e_{12}, \tag{4}$$

$$e_2' = e_2, \tag{5}$$

and the effective occupancy at any instant in state 1 and 2 can be given by

$$n_1' = n_1 [1 - e_{12}/(e_{12} + e_1 - e_2)], \tag{6}$$

$$n_2' = n_2 [1 + e_{12}/(e_{12} + e_1 - e_2)]. \tag{7}$$

The set of equations (1) and (2) is solved numerically using model parameters. The result of such a simulation is shown in Fig. 2(a), and the simulation parameter are presented in Table I. Note that the observed emission rates and effective emission rates are modified due to the occurrence of charge transfer even during emission. The reduction of occupancy for the fast state for a longer filling time, as seen in Fig. 2(a), is characteristic of this type of coupling.

B. Two distinct charge states

Here two different charge states of the same defect is considered. A schematic of this model is presented in Fig. 1(B), and the corresponding rate equations can be expressed as

$$\dot{n}_1 = -e_1 n_1 - e_2 n_2 + c_1 n (1 - n_1 - n_2) - c_2 n n_1, \tag{8}$$
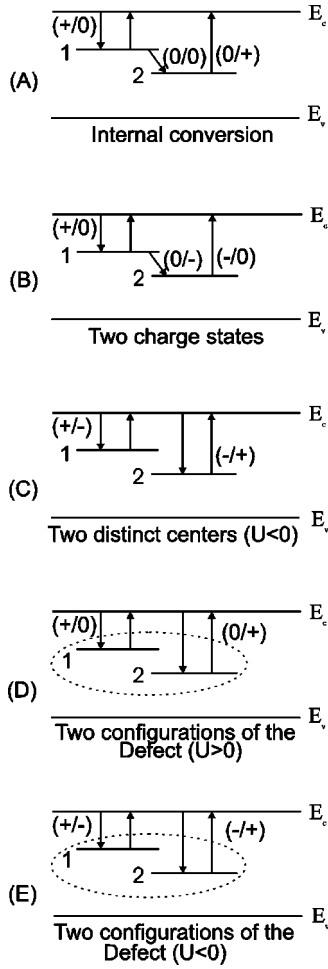
$$\dot{n}_2 = c_2 n n_1 - e_2 n_2, \tag{9}$$

FIG. 1. Schematics of five different models of coupling between two defect states 1 and 2, shown with the band diagram in silicon. A change in the charge state associated with an electronic transition is shown in brackets in each case.

where

$$n = 1 - n_1 - 2n_2. \tag{10}$$

Other symbols have their usual meaning as described in Fig. 1(A). Here state 1 is assumed to be a singly charged state, and state 2 refers to doubly charged state.

The result of simulation using Eqs. (8)–(10) is shown in Fig. 2(b). Here the defect states have been assumed to have a positive U, i.e. the second charge state is deeper than the first charge state. Note that the rate of increase of the occupancy of the higher charge state is proportional to the occupancy of the lower charge state. As a consequence, its occupancy increases with an effective time lag. A critical comparison of features with different models is presented in Sec. III.

C. Two distinct negative-U centers

Here we consider two distinct centers with concentrations N_{T1} and N_{T2}, and they are taken to be negative-U centers, i.e., their doubly charged state is shallower than the singly charged state. If the electron-phonon coupling is stronger than the Coulomb repulsion between two electrons, then negative U is favored.[18] Positive U refers to the positive difference in binding energies for singly and doubly occu-
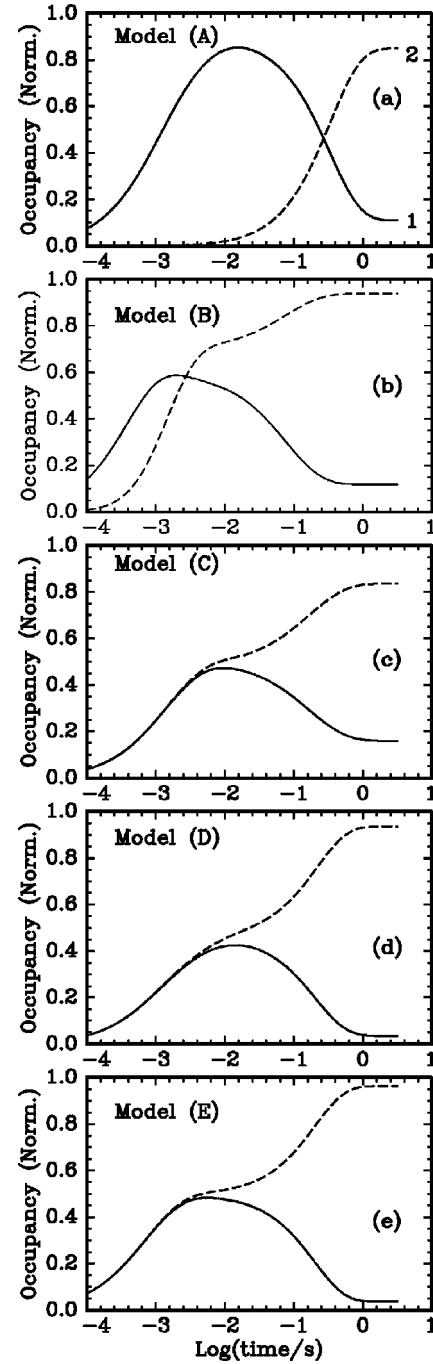

FIG. 2. Trap occupancy features as a function of time, for different models of coupling presented in Fig. 1. The parameter values used for simulation are mentioned in Table I.

pied charge states of the defect, considering only electron-electron interaction. The situation is schematically presented in Fig. 1(C). The corresponding rate equations can be written as

$$\dot{n}_1 = c_1 n (N_{T1}/N_T - n_1) - e_1 n_1, \tag{11}$$

$$\dot{n}_2 = c_2 n (N_{T2}/N_T - n_2) - e_2 n_2, \tag{12}$$

where

$$n = 1 - 2n_1 - 2n_2, \tag{13}$$

TABLE I. Various models of coupling for charge transfer among two defect states, with simulation parameters and some examples of physical systems reported in the literature.

Models of coupling	Simulation parameters (s^{-1})					Charge transfer	Examples with reference
	e_1	e_2	c_1	c_2	e_{12}		
Internal conversion	9.6	-	8×10^2	-	2.8	serial	Si (Ref. 23), $Al_xGa_{1-x}As$ (Ref. 22)
Two charge states	9.6	0.36	8×10^2	12×10^2	-	serial	Si (Ref. 24), $Al_xGa_{1-x}As$ (Ref. 27), InP (Ref. 10), etc.
Two distinct centers with $U<0$	9.6	0.36	8×10^2	12×10^2	-	parallel	$Al_xGa_{1-x}As$ (Ref. 30), Si (Ref. 29)
Two configurations with $U>0$	9.6	0.36	8×10^2	12×10^2	-	parallel	$Hg_yCd_{1-y}Te$ (Refs. 12 and 25), $Al_xGa_{1-x}As$ (Ref. 31)
Two configurations with $U<0$	9.6	0.36	8×10^2	12×10^2	-	parallel	Si (Ref. 15), this work

and total trap concentration $N_T=N_{T1}+N_{T2}$. The factor 2 in Eq. (13) appears due to the negative-U property of the defect.

The results of simulation are shown in Fig. 2(c). As depicted in Fig. 1(C), note that this model considers a parallel process of charge transfer between different states in contrast to the first two cases of serial process. In this model, if a large number of shallow donors is introduced, i.e., the condition of Eq. (13) is relaxed, then no charge transfer will be observed. The distinctive feature of this model in contrast to the models of Figs. 1(A) and 1(B) is the simultaneous growth of occupancy of states 1 and 2, and for filling times larger than the emission time constant of state 1, there is a marked growth of state 2 which is at the cost of decrease of occupancy of state 1, a faster emitting state.

D. Two configurations of a defect with $U>0$

Here it is assumed that the same defect can have multiple configurations, and it can switch between these configurations by emitting an electron from one configuration and capturing an electron into the other configuration. These configurations have been assumed to introduce positive-U levels [Fig. 1(D)]. The rate equations can be expressed as

$$\dot{n}_1=c_1n(1-n_1-n_2)-e_1n_1, \qquad (14)$$

$$\dot{n}_2=c_2n(1-n_1-n_2)-e_2n_2, \qquad (15)$$

where

$$n=1-n_1-n_2. \qquad (16)$$

The results of such simulations are shown in Fig. 2(d). Note that the occupancy features are similar to the results of Fig. 1(C), except the fact that there is substantial decrease in the occupancy of state 1 for larger filling time and the corresponding state 2 occupancy becomes very high; i.e., for large filling time all the states of configuration 2 are filled.

E. Two configurations of the defect with $U<0$

This model is identical with Fig. 1(D), but now with the two configurations introducing negative-U energy levels. The situation is schematically presented in Fig. 1(E). The relevant rate equations can be expressed as

$$\dot{n}_1=c_1n(1-n_1-n_2)-e_1n_1, \qquad (17)$$

$$\dot{n}_2=c_2n(1-n_1-n_2)-e_2n_2, \qquad (18)$$

where

$$n=1-2n_1-2n_2, \qquad (19)$$

The results are shown in Fig. 2(e). The occupancy features are very similar to those of Fig. 1(D) model.

III. DISCUSSION ON MODEL DISTINCTION

We have considered five different models of coupling between two defect states. The model parameters used for simulation are listed in Table I. In the first two cases, charge is essentially transferred through a hierarchical process[19] or serial process, whereas the last three models deal with parallel process of transfer. In each case of simulations, the common constraint we have assumed essentially is on the number of free carriers which is taken to be dependent on the number of ionized donor states. Except for model of Fig. 1(C), in all the models the coupling between the two states is inbuilt and thus charge transfer will be observed irrespective of the above constraint. In case of deep defect dominated materials, this constraint is naturally satisfied due to compensation effect, as in the case of silicon related DX center in $Ga_xAl_{1-x}As$,[20] damage-related compensating center in heavy-ion-implanted silicon,[21] etc.

A critical comparison of the characteristics of the simulated curves reveals that in the case of a serial model, initially the occupancy of the slow states is very low compared to the fast emitting state. This is in contrast to the parallel model, where individual occupancies are substantial even for short filling times irrespective of the emission rate. Thus it may be treated as a primary guide for model distinction in analyzing experimental data.

Note that the basic occupancy characteristics of all the three parallel models are quite similar. However, the model of Fig. 1(C), which is based on two distinct negative-U centers, is qualitatively different from the models of Figs. 1(D) and 1(E) in regard to the dependence of the model of Fig. 1(C) on the number of free carriers, as argued earlier. Moreover, it is to be noted that the reduction in occupancy at longer filling time for the fast state is substantial in the models of Figs. 1(D) and 1(E), compared to the model of Fig. 1(C). In a parallel mechanism, the electrons emitted from the fast state are recaptured into the slow state, and the relative occupancies of the two states in the short filling region is governed by the product of their respective capture rates and the probabilities of occurrence. However, in the steady state the slower state gains significantly at the cost of the faster

state, and occupancies are largely independent of capture and emission rates.

The models we discussed above have been invoked in various physical systems, especially in the study of defect metastability, which are often charge state controlled. The mechanism of the model of Fig. 1(A), i.e., internal conversion, was suggested for charge transfer between silicon DX states in $Al_xGa_{1-x}As$.[22] Multistable defect configurations and internal conversion between them have been reported for interstitial-carbon substitutional-group-V-atom pair defects in electron irradiated silicon.[23] Traps with two charge states which present strong coupling to the lattice have been observed in a variety of semiconductors, for example, in Si,[24] InP,[10] $Hg_yCd_{1-y}Te$,[25] GaAs,[26] and $Al_xGa_{1-x}As$,[27] which were mainly analyzed through DLTS studies without attempting such model formalism. As the DLTS technique is based on the temperature scanning method, inherent limitations of the spectral line shape due to a temperature-dependent prefactor in the capacitance transient, and the possible presence of a thermally activated capture process, may lead to a misinterpretation of the result. Such problems can be easily overcome by using single-shot measurements at a particular temperature, and by performing a spectroscopic analysis for isothermal transients taken for different filling times. Any isothermal transient spectroscopic technique will be more powerful to analyze such phenomena. We have recently demonstrated the use of TATS, an isothermal spectroscopic technique, in understanding the trapping kinetics of defects in heavily damaged silicon[28,29] and the DX center in $Al_xGa_{1-x}As$.[6]

Model of Fig. 1(C) has been suggested by several cluster calculations performed for DX centers in $Al_xGa_{1-x}As$.[30] A similar model was invoked recently in the study of charge redistribution among multiple traps in heavily damaged silicon.[29] Figure 1(D), i.e., a model of a defect with two different configurations, has been invoked in several studies.[12,13,25] Two defect configurations with positive U were suggested by Morgan[31] in a study of the DX center in $Ga_{1-x}Al_xAs$, whereas Su and Farmer[17] suggested negative-U configurations in their study on the same system. In addition to various studies on metastable defects using DLTS,[9] optical techniques have also been used to study metastable defects in electron irradiated Si.[32]

In general, though it is not straightforward to distinguish between serial and parallel kinetic models[33] due to the lack of a simple set of criteria, our simulation results provide a clear guideline to identify the suitability of a particular model in a real set of spectra. It is worth mentioning that for metastable defects, transformations occur among different configurations of the same defect, and the total concentration of the metastable defect is the sum of the concentration in each configuration. This total concentration is constant. The simple formalism presented for two defect states can be easily extended for a greater number of states as well. A combination of models can also be invoked in a real system of data.

IV. APPLICATION

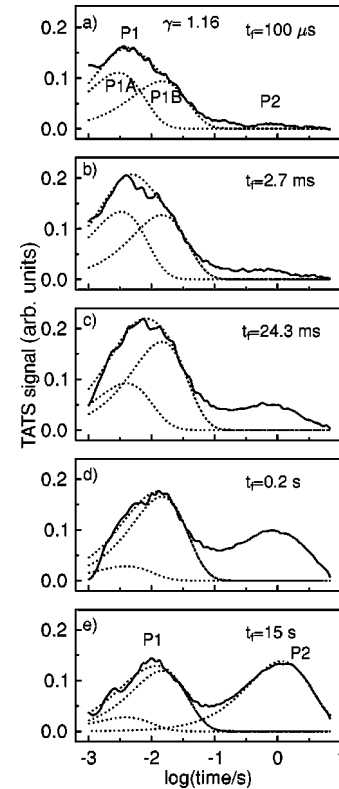In this section we will consider the applicability of the models discussed above to trapping kinetics data obtained

FIG. 3. First-order TATS spectra of ion-damaged n-Si at 217.6 K for different filling times (t_f), showing progressive changes in occupancy for a high dose (1×10^{14} cm^{-2}) Ar^+-implanted sample. Peak $P1$ is fitted (dotted line) with two different centers $P1A$ and $P1B$, and peak $P2$ is fitted to a Gaussian-broadened peak (the full width at half maximum is 25 meV) with separate dotted line in frame e.

for defects in heavily damaged silicon. The defects are created by MeV Ar^+-ion implantation with considerably high doses ($5 \times 10^{13} - 1 \times 10^{14}$ cm^{-2}), but below the amorphization threshold. More detailed information on experimental conditions and properties of the defects under consideration was reported elsewhere.[21,29,34] For as-implanted silicon, a conventional DLTS spectra shows the presence of a divacancy-related trap and a damage-related defect which has been ascribed to interstitial complex. To unravel any possible coupling between these defects, we performed a variable filling-pulse-width transient technique in the isothermal spectroscopic mode using TATS. To overcome the problems due to the high trap density and series resistance effect on a transient signal, a constant capacitance mode of operation was implemented using a feedback circuit, and voltage transients were used to monitor the trap occupancies for filling time over five orders of magnitude in time. Using higher-order TATS (see the Appendix), it was found that for lower filling times (t_f of the order of a few μs), the well-known divacancy-related peak constitutes two peaks whose occupancy changes nonmonotonically with filling time.[29] For a longer filling time, the peak height saturates, and constitutes only one peak which is usually attributed to divacancy trap.

In Fig. 3, we show a set of TATS spectra for progressively increasing filling times over five orders in magnitude ranging from 100 μs to 15 sec. Peak $P1$ is fitted (dotted
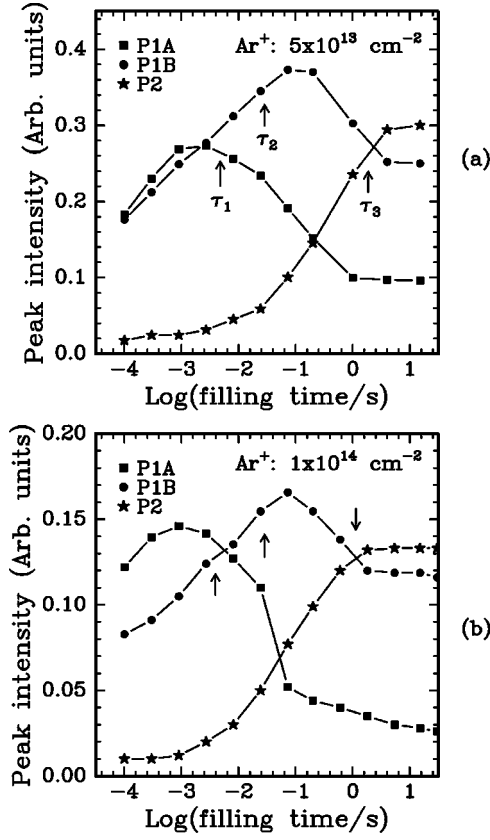
FIG. 4. Occupancy characteristics of individual peaks as a function of filling time for samples implanted with doses (a) 5×10^{13} cm^{-2} and (b) 1×10^{14} cm^{-2} of Ar$^+$ ions. Arrows indicate the measured emission time constants (τ) for the corresponding centers.

lines) to two emitting centers ($P1A$ and $P1B$) assuming a Gaussian broadening of 10 meV in activation energy for each of them. The time constant for each peak is obtained from experimental spectra for the high-filling-time limit. The occupancy of peak $P2$ increases monotonically, and saturates for a long filling time. The peak is fitted with a Gaussian broadening of 25 meV in activation energy, which is believed to result from a damage-induced strain surrounding the defects. The peak intensities obtained from such an analysis have been plotted as a function of the logarithm of filling time in Figs. 4(a) and 4(b) for samples implanted with two different doses. Peak $P1A$ initially increases, going through a maximum at a filling time approximately equal to its emission time constant. The increase of peak $P2$ occurs when, peak $P1A$ starts to decrease. Peak $P1B$ also goes through a maximum for longer filling times. These general features are common to samples irradiated with both high and low doses. Clearly this is a case of coupled carrier kinetics with multiple traps. Note that the apparent shift of peaks $P1A$ and $P1B$ is not due to any change in energy of the defect in question, but rather to a relative occupancy change of the constituent peaks.

In the light of the models discussed in Sec. III, there are *a priori* many possible-coupling mechanisms that can give rise to such features, viz. multiple-charge states of the same defect, an internal conversion from a metastable state to a stable state, different configurations of the same defect, etc. Before we attempt to pinpoint the mode of coupling among these defects, in the present case the key observation is that shallow states lose charges to deeper ones, when filling times are larger than their characteristic emission time. This suggests a redistribution of charges through multiple trapping. For filling times (t_f) shorter than the characteristic emission time (τ_e) of a particular level, the occupancy increases in proportion to the product of its capture constant and the number density of empty states. For $t_f > \tau_e$, emitted electrons from shallow states are recaptured by deeper states. The situation can be modeled using the following rate equation for three independent traps :

$$\dot{n}_i = -e_i n_i + c_i n (N_{Ti}/N_T - n_i), \quad i = 1-3, \qquad (20)$$

with a constraint on number of electrons as

$$n = \sum_{i=1}^{3} (N_{Ti}/N_T - n_i), \qquad (21)$$

where n_i is the concentration of occupied states for the ith, level with e_i and c_i its emission rate and capture constants, and N_{Ti} its total concentration. Equations (20) and (21) are normalized with respect to N_T. Results of numerical solutions of the above set of equations are shown in Fig. 5(a). We have used model parameters for N_{Ti} (with equal concentrations) and c_i and experimentally determined time constants (τ_e) for this simulation.

A distinctive feature of the occupancy data of this model, assuming independent states, is that the final equilibrium concentration (normalized) of the fastest trap ($P1A$) is not as low as the one seen in the experimental occupancy feature (see Fig. 4). It is also found that this feature is not merely dependent on the choice of capture and emission parameters, but is an essential characteristic of these sets of equations. This suggests that the fastest peak ($P1A$) and the slowest peak ($P2$) may not be independent, as we have assumed. Hence we modify the above model to include the assumption that peaks $P1A$ and $P2$ are two different configurations of the same defect. This additional constraint modifies the above rate equations as follows :

$$\dot{n}_1 = c_1 n((N_{T1} + N_{T3})/N_T - n_1 - n_3) - e_1 n_1, \qquad (22)$$

$$\dot{n}_2 = c_2 n(N_{T2}/N_T - n_2) - e_2 n_2, \qquad (23)$$

$$\dot{n}_3 = c_3 n((N_{T1} + N_{T3})/N_T - n_1 - n_3) - e_3 n_3, \qquad (24)$$

with the constraint on number of electrons as

$$n = 1 - n_1 - n_2 - n_3. \qquad (25)$$

Figure 5(b) shows the occupancy behavior in such a case, assuming the same emission and capture time constants as in the earlier case. Here we have assumed that $N_{T1} + N_{T3} = 0.5 N_T$ and $N_{T2} = 0.5 N_T$. This occupancy feature closely resembles those of experimental features of Fig. 4, particularly relating the reduction of occupancy of peak $P1A$ for longer filling times. Hence the defect related to peak $P1A$ can be considered an unstable configuration of defect $P2$; for higher filling times, configuration $P2$ dominates. A more careful comparison of Figs. 4 and 5(b) reveals that in the simulated curves, the reduction of peak $P1B$ for longer fill-
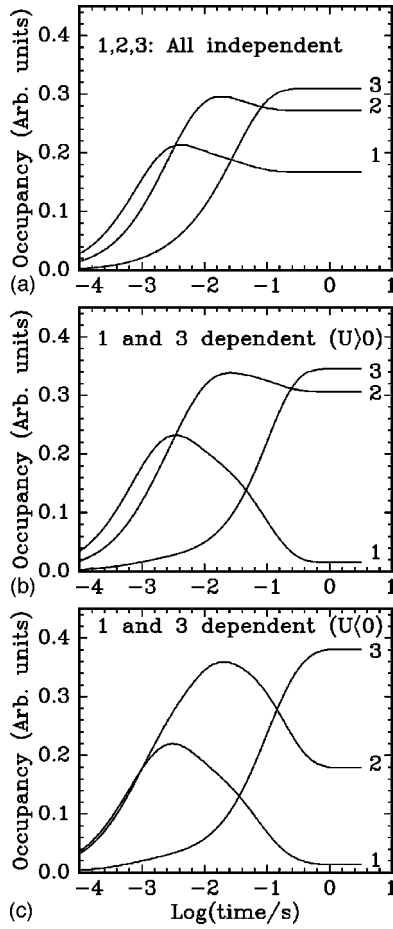
FIG. 5. Simulated occupancy characteristics of three trap levels found by solving rate equations under the condition $N_T > n$ (a) assuming three independent trap levels with equal concentrations; (b) assuming that are fastest and slowest states are two configurations of the same defect, with $U > 0$; (c) two configurations with $U < 0$. Parameters used for the simulations are $c_1 = 1000$, $c_2 = 400$, $c_3 = 80$, $e_1 = 200$, $e_2 = 40$, and $e_3 = 0.7$ (all in s^{-1} units).

ing times is not as large as seen in the experimental data. For a more accurate description of the coupling among these three defects, we assume that defects related to peaks $P1A$ and $P2$ introduce negative-U levels into the band gap. In this case, the rate equation of Eqs. (22)–(24) remains the same, except, for the constraint on the number of electrons [Eq. (25)] which will be modified as

$$n = 1 - 2n_1 - n_2 - 2n_3. \qquad (26)$$

The result of this analysis is shown in Fig. 5(c) which matches very well with the experimental features. It can be noted that the growth of peak $P2$ is primarily at the cost of peak $P1A$, while peak $P1B$ also contributes to growth of peak $P2$ for a filling time longer than its characteristic emission time. Thus our simulation shows that a proper description of the coupling among peaks $P1A$, $P1B$, and $P2$ can be made by assuming that peaks $P1A$ and $P2$ are two configurations of the same defect having negative-U character. The negative U could arise due to a strong coupling of the defect to the lattice relaxation and vibration. In analogy with the case of the DX center in Al$_x$Ga$_{1-x}$As, it is quite plausible that the fast state (peak $P1A$) could be due to a unrelaxed

configuration of the defect, while the slow state (peak $P2$) is a relaxed configuration of the same defect. Negative-U behavior has been argued to be consistent with a large lattice relaxation model in the case of a DX center.[35] We anticipate small interstitial clusters to behave as negative-U centers possibly along with large lattice relaxation. Further, a charge redistribution among multiple states, as observed here, is consistent with the framework of a broken bond negative-U model which incorporates a large lattice relaxation model, which has been argued in the case of a DX center.[17] Isolated interstitial Si (Si$_i^+$, Si$_i^0$) has been predicted to have a negative-U behavior, and possesses metastability due to its on- or off-center position in the lattice.[36] As the defect responsible is believed to be a self-interstitial cluster, it may involve a substantial lattice relaxation in the formation of a stable structure of this defect, and may give rise to negative-U behavior. However, a more direct verification of this negative-U behavior can come from low-temperature photoconductivity studies.[37]

The condition of Eqs. (21) or (25) is clearly satisfied in our experiment in the region of heavy damage. We not only have a large number of traps, but also the region is converted to a highly compensated region.[21] Also, note that the time scale of the dynamics is considerably slow due to the limited availability of free carriers in the damaged region, enabling capture measurements on a convenient time scale. For example, in the case of a divacancy level whose capture cross section is 3×10^{-15} cm^2, the filling time in the normal case with a free-carrier concentration of 1×10^{15} cm^{-3} would be of the order of a few tens of nanoseconds. In the damaged region, however, the carrier concentration is down to near-intrinsic levels, and hence the dynamics is slowed down to a millisecond scale.

Charge redistribution among multiple traps was observed in the case of a silicon-related DX center in Al$_x$Ga$_{1-x}$As.[17,6] In hydrogenated amorphous silicon, the process of charge redistribution from shallower to deeper states distributed exponentially in energy was invoked[38] in interpreting trapping kinetics data which were originally explained to be due to a progressive deepening of emission energy states during capture due to a defect relaxation process.[39] Here we provide a clean demonstration of charge redistribution among coupled defect levels. The major defect in as-implanted silicon was found to exist in two different configurations, and the shallower state is an unstable configuration, observable at lower filling times.

Defects created by electron irradiation in Si produce a variety of metastable defects, most of which are related to interstitial defects.[40,32,41] In contrast to the case of electron irradiation, MeV heavy-ion irradiation generates a large number of interstitials, which can migrate and agglomerate to form stable clusters. From a more detailed investigation of electrical properties of these defects in as-implanted and low-temperature annealed silicon, we have proposed that these defects are primarily related to interstitial clusters.[34] Though a detailed understanding of cluster behavior is lacking at present in the literature, recent theoretical studies on defect clusters (e.g., vacancy and interstitial clusters) have made several predictions about the total energy, relaxed atomic configurations, electronic structure etc.[42,43] Ground-state energy calculations of various interstitial clusters predict that a

four-interstitial (I_4) is a stable structure with a reasonably low energy.[43] Though there has been a lack of consensus about the electrical signature of stable defect clusters from theoretical predictions, recent experimental studies by Benton and co-workers[44,45] on self ion-implanted and annealed silicon shows that a number of electrically active states related to interstitial clusters are introduced in the band gap of both *n*- and *p*-type silicon. We believe that the dominant electrically active defect peak ($P2$) observed in our experiment is due to interstitial clusters of small size. These clusters eventually give rise to well-known {311} defects during annealing.[46,47] The cluster binding energy is known to change with the size of the clusters, and this might be reflected in the activation energy of the associated defect. The sensitivity of the trap activation energy to the processing condition[21] as a result of a change in the cluster size distribution and the degree of disorder in the defect surrounding is also an indication in support of this. Here it is important to emphasize the importance of using a single-shot isothermal spectroscopic technique such as TATS in monitoring the relative trap occupancy, and in arriving at a particular model of charge transfer. In temperature scanning spectroscopy, such as DLTS, a sensitivity of signal to filling time and its temperature dependence can lead to erroneous conclusions.

V. CONCLUSION

We have presented a comprehensive analysis of several simple models of coupled trapping kinetics among multiple defect states, monitored in a typical capacitance transient spectroscopic measurement of charge occupancy. Assuming two defect levels coupled through a common constraint of free-carrier density, we solve coupled differential equations governing their trapping and detrapping kinetics, and derive the relative occupancy of each state as a function of time. The occupancy features of five different models have been critically assessed, with a view toward setting a criterion for model distinction in real systems. We successfully apply our analysis in studying kinetics of charge relaxation from defects in heavily damaged silicon. We demonstrate the occurrence of charge redistribution among multiple defects in as-implanted silicon. From a careful analysis of the occupancy features of experimental data and data obtained from simulation assuming three defect states, it was found that the major defect is a stable configuration of another shallower metastable state. A closer match with experimental features could be obtained if the two interdependent states are assumed to possess negative-*U* behavior. The major defect is believed to be related to a small interstitial cluster where metastability may result from many-body relaxation process. The model formulation presented here can be easily extended to a more complex system using a combination of these simple models.

APPENDIX

Time analyzed transient spectroscopy (TATS)[3] is an isothermal spectroscopy in the time domain. It is analogous to DLTS, which is in the temperature domain. The first- (S_1) and second order (S_2) TATS signals are given by.

$$S_1(t) = C(t) - C[(1+\gamma)t], \tag{A1}$$

$$S_2(t) = C(t) - 1.5C[(1+\gamma)t] + 0.5C[(1+\gamma)^2 t]1, \tag{A2}$$

where $C(t)$ is the capacitance transient, and γ is a selectable experimental constant defining moving rate window. For an exponential transient with a time constant τ, $S(t)$ has a maximum when plotted against $\ln(t)$, and it occurs at a time t_m given by

$$\tau = \left[\frac{\gamma}{\ln(1+\gamma)} \right] t_m. \tag{A3}$$

The peak value of the TATS signal is a measure of the strength of the exponential. One of the principal advantages of time domain spectroscopy such as TATS is that the line shape of a peak is independent of the trap parameters or the range of time and temperature. Other advantages include the straightforwardness of the analysis for a non-Debye trap signature, and its suitability for studying trapping kinetics at a fixed temperature.

*Email: pkgiri@igcar.ernet.in

[1] D.V. Lang, J. Appl. Phys. **77**, 3023 (1974).

[2] See, e.g., H. Okusi and Y. Takumaru, Jpn. J. Appl. Phys. **19**, L335 (1990); P.M. Henry, J.M. Meese, J.W. Farmer, and C.D. Lamp, J. Appl. Phys. **57**, 628 (1985).

[3] S. Agarwal, Y.N. Mohapatra, and V.A. Singh, J. Appl. Phys. **77**, 3155 (1995).

[4] G.D. Watkins, Mater. Sci. Forum **38-41**, 39 (1989).

[5] M. Levinson, J.L. Bento, and L.C. Kimerling, Phys. Rev. B **27**, 6216 (1983).

[6] S. Agarwal, Y.N. Mohapatra, V.A. Singh, and R. Sharan, J. Appl. Phys. **77**, 5725 (1995).

[7] W. Schroter, J. Kronewitz, U. Gnauert, F. Riedel, and M. Sbeit, Phys. Rev. B **52**, 13 726 (1995).

[8] See, e.g., L. Dobaczewski and J.M. Langer, Mater. Sci. Forum **65-66**, 433 (1990).

[9] J.L. Benton, J. Electron. Mater. **18**, 199 (1989).

[10] M. Levinson, M. Stavola, P. Besoni, and W.A. Bonner, Phys. Rev. B **30**, 5817 (1984).

[11] B. Hamilton, A.R. Peaker, and S.T. Pantelides, Phys. Rev. Lett. **61**, 1627 (1988).

[12] G. Zoth and W. Schroter, Philos. Mag. **58**, 623 (1988).

[13] J.F. Barbot, I.A. Hummelgen, P. Girault, and C. Blanchard, J. Mater. Sci. **30**, 3471 (1995).

[14] J.D. Weeks, J.C. Tully, and L.C. Kimerling, Phys. Rev. B **12**, 3286 (1975).

[15] W.M. Chen, J.H. Svensson, E. Janzen, B. Monemar, and A. Henry, Phys. Rev. Lett. **71**, 416 (1993).

[16] I.A. Hummelgen and W. Schroter, Appl. Phys. Lett. **62**, 2703 (1993).

[17] Z. Su and J.W. Farmer, Appl. Phys. Lett. **59**, 1746 (1991).

[18] P.W. Anderson, Phys. Rev. Lett. **34**, 953 (1975).

[19] R.G. Palmer, D.L. Stein, E. Abrahams, and P.W. Anderson, Phys. Rev. Lett. **53**, 958 (1984).

[20] See, e.g., P.M. Mooney, J. Appl. Phys. **67**, R1 (1990).

[21] P.K. Giri and Y.N. Mohapatra, Appl. Phys. Lett. **71**, 1628 (1997).

[22] S. Agarwal, Ph.D. thesis, IIT Kanpur, India, 1995.

[23] X.D. Zhan and G.D. Watkins, Phys. Rev. B **47**, 6363 (1993).

[24] R.D. Harris, J.L. Newton, and G.D. Watkins, Phys. Rev. Lett. **48**, 1271 (1982).

[25] M. Koehler, E.F. Ferrari, J.F. Barbot, and I.A. Hummelgen, Phys. Rev. B **53**, 7805 (1996).

[26] S.T. Lai, D. Alexiev, and B.D. Nener, J. Appl. Phys. **78**, 3686 (1995).

[27] L. Dobaczewski and P. Kaczor, Semicond. Sci. Technol. **6**, B51 (1991).

[28] P.K. Giri, S. Dhar, V.N. Kulkarni, and Y.N. Mohapatra, J. Appl. Phys. **81**, 260 (1997).

[29] P.K. Giri, S. Dhar, V.N. Kulkarni, and Y.N. Mohapatra, Phys. Rev. B **57**, 14 603 (1998).

[30] R. Jones and O. Oberg, Phys. Rev. B **44**, 3407 (1991).

[31] T.N. Morgan, Phys. Rev. B **34**, 2664 (1986).

[32] J.H. Svensson and B. Monemar, Phys. Rev. B **40**, 1410 (1989).

[33] J.R. Macdonald, J. Appl. Phys. **62**, R51 (1987).

[34] P.K. Giri and Y.N. Mohapatra, J. Appl. Phys. **84**, 1901 (1998).

[35] D.J. Chadi and K.J. Chang, Phys. Rev. Lett. **61**, 873 (1988); Phys. Rev. B **39**, 10 366 (1989).

[36] G.D. Watkins, Semicond. Sci. Technol. **6**, B111 (1991).

[37] K.A. Khachaturyan, D.D. Awschalom, J.R. Rozen, and E.R. Weber, Phys. Rev. Lett. **63**, 1311 (1989).

[38] J.W. Farmer and Z. Su, Phys. Rev. Lett. **71**, 2979 (1993).

[39] J. David Cohen, Thomas M. Leen, and Randall J. Rasmussen, Phys. Rev. Lett. **69**, 3358 (1992).

[40] C.A. Londos, Phys. Rev. B **34**, 1310 (1986).

[41] O.O. Awadelkarim, W.M. Chen, H. Weman, and B. Monemar, Phys. Rev. B **41**, 1019 (1990).

[42] J.L. Hastings, S.K. Estricher, and P.A. Fedders, Phys. Rev. B **56**, 10 215 (1997).

[43] N. Arai, S. Takeda, and M. Kohyama, Phys. Rev. Lett. **78**, 4265 (1997).

[44] J.L. Benton, S. Libertino, P. Kringhoj, D.J. Eaglesham, J.M. Poate, and S. Coffa, J. Appl. Phys. **82**, 120 (1997).

[45] J.L. Benton, K. Halliburton, S. Libertino, D.J. Eaglesham, and S. Coffa, J. Appl. Phys. **84**, 4749 (1998).

[46] J. Kim, J.W. Wilkins, F.S. Khan, and A. Canning, Phys. Rev. B **55**, 16 186 (1997).

[47] J. Kim, F. Kirchhoff, J.W. Wilkins, and F.S. Khan, Phys. Rev. Lett. **84**, 503 (2000).